Cell PRESS

Regulation of N-type Voltage-Gated Calcium Channels and Presynaptic Function by Cyclin-Dependent Kinase 5

Susan C. Su,[1,2] Jinsoo Seo,[1,2] Jen Q. Pan,[4] Benjamin Adam Samuels,[1,2] Andrii Rudenko,[1,2] Maria Ericsson,[5] Rachael L. Neve,[3] David T. Yue,[6] and Li-Huei Tsai[1,2,4,*]
[1]The Picower Institute for Learning and Memory, Department of Brain and Cognitive Sciences
[2]Howard Hughes Medical Institute
[3]McGovern Institute for Brain Research, Department of Brain and Cognitive Sciences
Massachusetts Institute of Technology, Cambridge, MA 02139, USA
[4]Stanley Center for Psychiatric Research, Broad Institute, Cambridge, MA 02142, USA
[5]Department of Cell Biology, Harvard Medical School, Boston, MA 02115, USA
[6]Department of Biomedical Engineering, The Solomon H. Snyder Department of Neuroscience, Johns Hopkins School of Medicine,
Johns Hopkins University, Baltimore, MD 21205, USA
*Correspondence: lhtsai@mit.edu
http://dx.doi.org/10.1016/j.neuron.2012.06.023

SUMMARY

N-type voltage-gated calcium channels localize to presynaptic nerve terminals and mediate key events including synaptogenesis and neurotransmission. While several kinases have been implicated in the modulation of calcium channels, their impact on presynaptic functions remains unclear. Here we report that the N-type calcium channel is a substrate for cyclin-dependent kinase 5 (Cdk5). The pore-forming α_1 subunit of the N-type calcium channel is phosphorylated in the C-terminal domain, and phosphorylation results in enhanced calcium influx due to increased channel open probability. Phosphorylation of the N-type calcium channel by Cdk5 facilitates neurotransmitter release and alters presynaptic plasticity by increasing the number of docked vesicles at the synaptic cleft. These effects are mediated by an altered interaction between N-type calcium channels and RIM1, which tethers presynaptic calcium channels to the active zone. Collectively, our results highlight a molecular mechanism by which N-type calcium channels are regulated by Cdk5 to affect presynaptic function.

INTRODUCTION

Calcium channels in the Ca$_V$2 voltage-gated calcium channel family are enriched in neurons and are composed of multiple subunits. The α_{1B} subunit encodes the pore-forming subunit of N-type calcium channels (Ca$_V$2.2) (Westenbroek et al., 1992). In addition to their well-established roles in spinal nociception and neuropathic pain signaling mediated by G$\beta\gamma$ G-protein subunits (Snutch, 2005), N-type calcium channels contribute to synaptic transmission in the hippocampus (Catterall and Few,

2008). Together with the P/Q-type calcium channels, these two major classes of presynaptic calcium channels are sufficient to account for synaptic transmission at the hippocampal CA3-CA1 synapse (Luebke et al., 1993; Wheeler et al., 1994).

N-type calcium channels play a prominent role in neurotransmitter release and directly bind several key synaptic transmission proteins. The intracellular domain between the II-III loops of the Ca$_V$2.2 pore-forming α_1 subunit is known as the synaptic protein interaction (synprint) region (Sheng et al., 1994). The synprint region binds syntaxin and synaptotagmin, two important components of the SNARE complex (Sheng et al., 1998). Synaptic transmission at the presynaptic terminal involves calcium influx, which triggers vesicle fusion and exocytosis by the "zippering" of SNARE proteins with the plasma membrane (Jahn et al., 2003). The synprint region of Ca$_V$2.2 is also a binding site for the active-zone protein RIM1 (Coppola et al., 2001). RIM1 can interact with the β auxiliary subunit of P/Q-type calcium channels to suppress inactivation, allow calcium influx, and facilitate synaptic vesicle docking to the active zone (Kiyonaka et al., 2007). Furthermore, RIM1 directly binds the C-terminal regions of the α_1 subunit of both N- and P/Q-type calcium channels, and it tethers these channels to presynaptic terminals in order to facilitate synchronous transmitter release (Han et al., 2011; Kaeser et al., 2011). The interaction between N-type calcium channels and SNARE complex proteins is significant, because kinases, such as protein kinase C (PKC) and calcium calmodulin-dependent kinase II (CaMKII), phosphorylate the II-III loop of the calcium channel, which affects the N-type calcium channel interaction with various components of the SNARE complex and impacts neurotransmitter release (Yokoyama et al., 1997). However, it remains unknown whether other kinases play a role in modulating N-type calcium channel function. Recently, the scaffolding molecule CASK, which contains a binding domain for N-type calcium channels, was identified as a cyclin-dependent kinase 5 (Cdk5) substrate (Samuels et al., 2007). Upon phosphorylation by Cdk5, CASK increases its interaction with N-type calcium channels to regulate synaptogenesis.

Cdk5 is a proline-directed serine/threonine kinase that is highly expressed in postmitotic cells of the central nervous system and requires its binding partner, p35, for activity (Chae et al., 1997; Tsai et al., 1994). Cdk5-mediated phosphorylations of a wide variety of substrates highlights its diverse roles in neuronal functions, including migration (Ohshima et al., 1996), cytoskeletal dynamics (Fu et al., 2007), synaptic vesicle cycle (Tan et al., 2003), and synaptic plasticity (Guan et al., 2011). Under excitotoxic conditions, calcium influx through the NMDA receptors activates the calcium-dependent protease calpain to cleave p35 to p25, which in turn hyperactivates Cdk5 (Lee et al., 2000; Patrick et al., 1999). The Cdk5/p25 complex has been implicated in neurodegenerative diseases, including Alzheimer's disease (Su and Tsai, 2011).

Recent evidence suggests that Cdk5 plays a critical role in regulating synapse formation (Cheung et al., 2007) and in synaptic scaling (Seeburg et al., 2008). Additionally, Cdk5 is proposed to be a major regulator of neurotransmitter release by regulating the size of the synaptic vesicle pool (Kim and Ryan, 2010), and it has also been implicated in the modification of synaptic connectivity and strength of hippocampal CA3 recurrent synapses (Mitra et al., 2011). However, the Cdk5 substrates directly responsible for neurotransmitter release are still poorly understood. Cdk5 was previously demonstrated to phosphorylate an intracellular domain of presynaptic P/Q-type calcium channels (Tomizawa et al., 2002). As a consequence of this phosphorylation event, neurotransmitter release is decreased due to the dissociation of P/Q-type calcium channels from the SNAP-25 and synaptotagmin complex.

Although several kinases have been implicated in phosphorylating and thereby affecting the binding of voltage-gated calcium channels to various synaptic proteins, no specific mechanisms have been elucidated by which a particular kinase regulates calcium channels to ultimately impact neurotransmitter release and presynaptic plasticity. Here we demonstrate that the N-type voltage-gated calcium channel, a major presynaptic calcium channel, is a Cdk5 substrate. Phosphorylation of the $Ca_V2.2$ pore-forming α_1 subunit by Cdk5 increases calcium influx by enhancing channel open probability and also facilitates neurotransmitter release. These events are mediated by an interaction between $Ca_V2.2$ and RIM1, which impacts vesicle docking at the active zone. Our results outline a mechanism by which Cdk5 regulates N-type calcium channels and affects presynaptic function.

RESULTS

The N-type Calcium Channel Is a Cdk5 Substrate

To investigate whether the N-type calcium channel is a Cdk5 substrate, we cloned the intracellular domains of the $Ca_V2.2$ α_1 subunit into glutathione S-transferase (GST) fusion protein constructs for in vitro kinase assays (Figure 1A). Each purified GST-$Ca_V2.2$ protein fragment was incubated with an activated Cdk5/p25 protein complex along with radioactive [γ32-P]ATP to assay the level of Cdk5 kinase activity (Figure 1B). Two GST-$Ca_V2.2$ fusion protein fragments, the C-terminal 3 (CT 3, amino acids 1981–2120) and C-terminal 4 fragments (CT 4, amino acids 2121–2240) were consistently phosphorylated by Cdk5 (Fig-

ure 1C). Mutagenesis of serine 2013 (S2013), a consensus Cdk5 site on the CT 3 fragment, to alanine abolished Cdk5 phosphorylation. However, several combinations of point mutations on the CT 4 fragment were insufficient to reduce Cdk5/p25 phosphorylation (Figure S1 available online). Only mutagenesis of all seven putative Cdk5 phosphorylation sites on the CT 4 fragment resulted in undetectable phosphorylation levels (Figure 1D). These kinase assays identify the N-type calcium channel as a Cdk5 substrate.

The N-type Calcium Channel Is Phosphorylated by Cdk5 In Vivo

To confirm phosphorylation of the N-type calcium channel, we generated and purified a phosphorylation-state-specific antibody to S2013, a well-conserved residue (Figure 2A). The phospho-$Ca_V2.2$ antibody (p$Ca_V2.2$) signal was robust when the CT 3 fragment, but not the CT 3 (S2013A) fragment, was coincubated with Cdk5/p25, indicating that the antibody was specific to S2013-phosphorylated $Ca_V2.2$ in vitro (Figure S2). Furthermore, the p$Ca_V2.2$ antibody signal was observed only in the presence of Cdk5/p35 in a cell line stably expressing the rat isoform of $Ca_V2.2$ (Lin et al., 2004), and alkaline phosphatase (CIP) treatment abolished the signal (Figure 2B). Since S2013 is also conserved in P/Q-type calcium channels, we tested the specificity of the Cdk5-dependent S2013 phosphorylation by immunoprecipitation of brain lysates with an anti-$Ca_V2.2$ antibody, followed by immunoblotting for p$Ca_V2.2$ in lysates of control and Cdk5 conditional knockout (cKO) mice (Guan et al., 2011). We noted that p$Ca_V2.2$ levels were significantly reduced in forebrain lysates of adult Cdk5 cKO mice, providing in vivo evidence that the N-type calcium channel is a Cdk5 substrate (Figure 2C).

Increased N-type Calcium Current Density as a Consequence of Cdk5-Mediated Phosphorylation

To examine the functional significance of Cdk5-mediated phosphorylation of $Ca_V2.2$ on the biophysical properties of the channel, we conducted whole-cell recordings in heterologous tSA-201 cells transfected with either the full-length wild-type human $Ca_V2.2$ α_1 subunit (WT $Ca_V2.2$) or the phosphorylation mutant $Ca_V2.2$ α_1 subunit, in which all eight Cdk5 phosphorylation sites in the C-terminal region were abolished (8X $Ca_V2.2$), in addition to the obligatory $\beta3$ and $\alpha2\delta$ auxiliary subunit cDNAs. Using 5 mM barium as the charge carrier, we found that the expression of WT $Ca_V2.2$ elicited canonical voltage-gated N-type currents. The phosphorylation mutant 8X $Ca_V2.2$ expressed a current-density profile similar to that of WT $Ca_V2.2$. Remarkably, following coexpression with Cdk5/p35, the WT $Ca_V2.2$ peak current amplitude and current density were significantly increased compared to those of WT $Ca_V2.2$ alone (Figures 3A and 3B; Table S1). In contrast to WT $Ca_V2.2$ however, cells transfected with 8X $Ca_V2.2$ in the presence of Cdk5/p35 did not display an increase in N-type current density (Figures 3A and 3B). In a cell line stably expressing the rat isoform of $Ca_V2.2$ (Lin et al., 2004), phosphorylation of $Ca_V2.2$ by Cdk5/p35 also dramatically increased N-type current density, providing independent support that the increase in N-type current density is mediated by Cdk5 phosphorylation (Figures S3A and S3B; Table S2). There were no differences in activation kinetics or voltage dependence of activation between the WT $Ca_V2.2$ and 8X
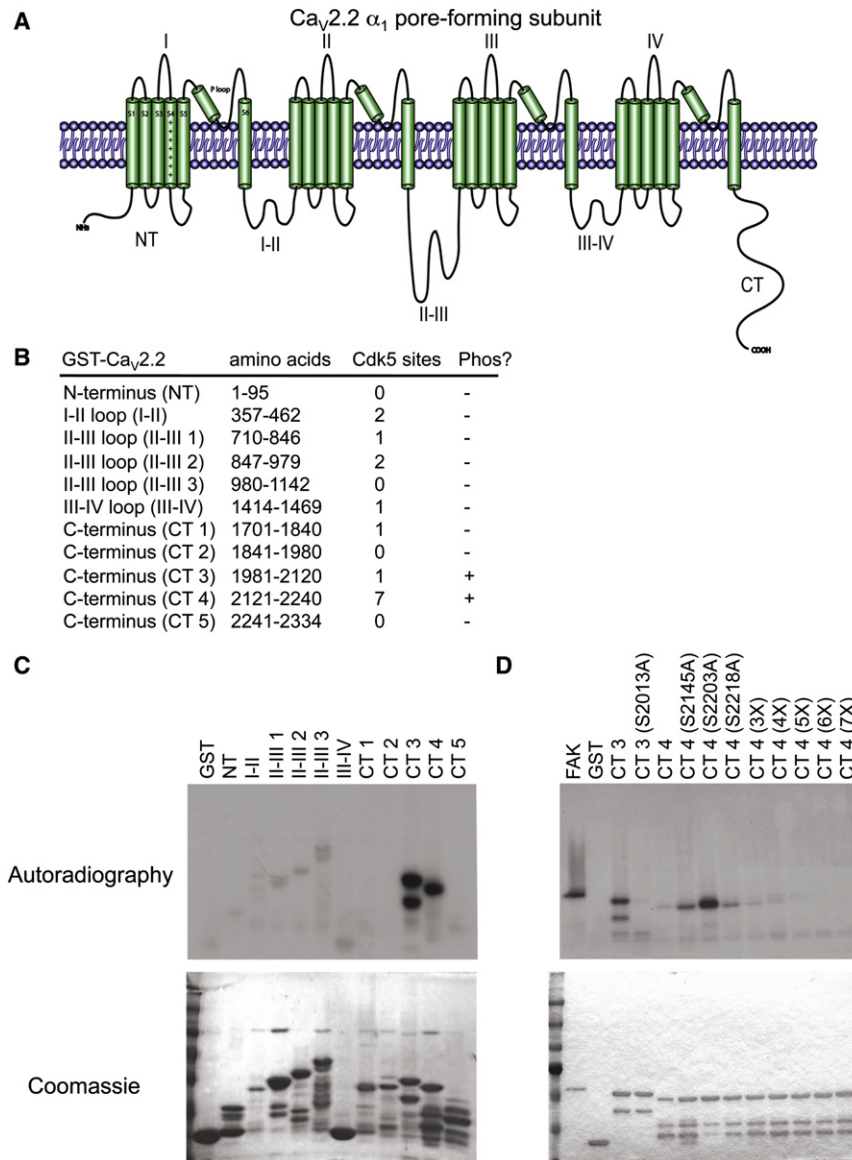
Figure 1. Phosphorylation Mapping of the N-type Calcium Channel In Vitro

(A) Schematic of the N-type voltage-gated calcium channel α_1 pore-forming subunit. The α_1 subunit is the functional core of the voltage-gated calcium channel containing the gating mechanisms, toxin-binding domains, and ion-conducting pore. Voltage-gated calcium channels form heteromeric subunit complexes consisting of the pore-forming α_1 subunit and auxiliary β, $\alpha_2\delta$, and γ subunits.

(B) Diagram of the various GST fusion protein constructs. The intracellular domains spanning the entire Ca$_V$2.2 α_1 subunit were cloned into GST fusion protein constructs (GST-Ca$_V$2.2).

(C) GST-Ca$_V$2.2 fragments were subjected to an in vitro kinase assay with purified Cdk5/p25. The C-terminal fragments 3 and 4 (CT 3 and CT 4) were phosphorylated by autoradiography (top). GST-Ca$_V$2.2 proteins expression as revealed by Coomassie staining (bottom).

(D) Mutagenesis of the single Cdk5 consensus site on the CT 3 fragment (S2013A) abolished Cdk5 phosphorylation. A combination of serine/threonine to alanine point mutations at Cdk5 phosphorylation sites dramatically decreased Cdk5/p25 phosphorylation of the CT 4 fragment. Sequential mutations were generated from the C terminus end (7X represents all the combination of seven phosphorylation mutations spanning CT 4). GST, negative control; FAK, positive control. See also Figure S1.

Cdk5 Plays a Critical Role in Regulating Channel Open Probability of Ca$_V$2.2

In addition to the effects of Cdk5/p35 on steady-state inactivation, we reasoned that a distinct mechanism must underlie the dramatic increase in Ca$_V$2.2 current density following Cdk5/p35-mediated phosphorylation. Previous reports have indicated a role for scaffolding proteins in the modulation of calcium channels and enhanced calcium influx due to increased channel surface expression (Brittain et al., 2009; Lai et al., 2005; Leenders et al., 2008). Accordingly, we conducted cell-surface biotinylation assays to examine whether Cdk5/p35 increases Ca$_V$2.2 surface expression in our heterologous system. However, Ca$_V$2.2 surface expression was not upregulated by Cdk5/p35 in stable cell lines or after coexpression with WT Ca$_V$2.2 or 8X Ca$_V$2.2, indicating that altered channel surface expression was not responsible for the enhancement of the Ca$_V$2.2 current density by Cdk5/p35-mediated phosphorylation (Figures 4A and 4B; Table S3). We next assessed channel open probability (P$_o$) of Ca$_V$2.2 in the presence of Cdk5/p35 as previously described (Agler et al., 2005). To obtain maximal channel open probability, P$_o$, for each cell, the maximal ionic current conductance, G$_{max}$ (Figure 4C), was plotted as a function of the integral of the channel gating current at the reversal potential Q$_{max}$ (Figure 4D). Interestingly, Cdk5/p35-mediated

Ca$_V$2.2 channels in the presence or absence of Cdk5/p35 (Figures 3C, 3D, S3C, and S3D). In examining inactivation kinetics, cotransfection with Cdk5/p35 increased the WT Ca$_V$2.2 inactivation time constant at the first test potential; however, the presence of Cdk5/p35 did not affect the inactivation kinetics of the 8X Ca$_V$2.2 channel at three different test potentials (Figures 3E and S3E). In steady-state inactivation (SSI) profiles, WT Ca$_V$2.2 demonstrated a greater availability of channels for opening in the presence of Cdk5/p35, as denoted by the rightward shift of the SSI curve (Figures 3F and S3F). Taken together, these data indicate that phosphorylation of Ca$_V$2.2 by Cdk5 increases the availability of calcium channels. Notably, there were no differences in SSIs at the holding potential at which N-type current density was measured (-100 mV), suggesting that differences in channel availability cannot account for the increased N-type current density mediated by Cdk5 phosphorylation.
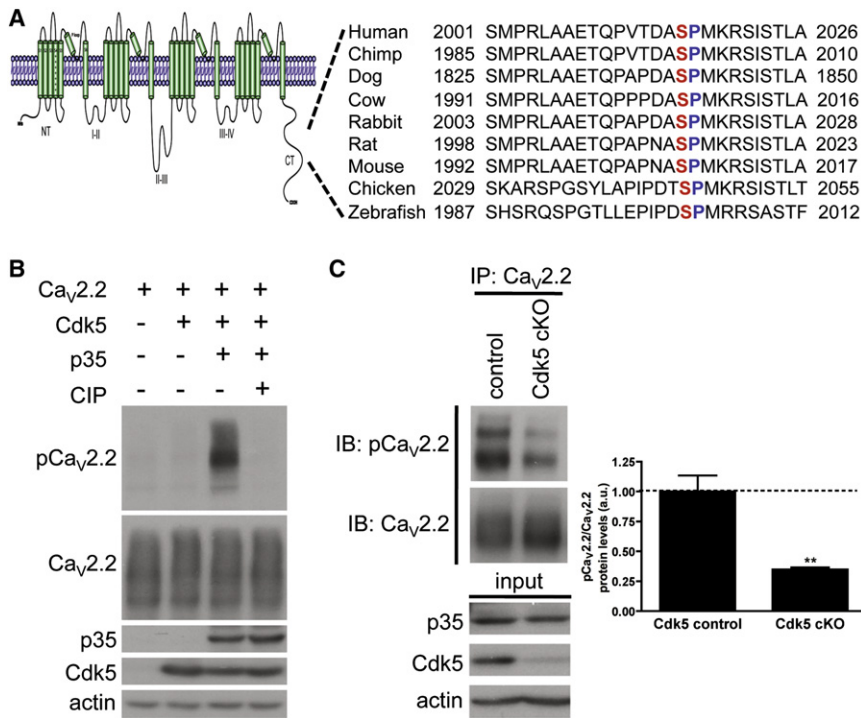
Figure 2. Phosphorylation of the N-type Calcium Channel In Vivo at Serine-2013

(A) Serine-2013 (S2013) is a highly conserved residue on the C-terminal domain of the N-type calcium channel α_1 subunit.

(B) Verification of the specificity of the phospho-specific antibody pCaV2.2 in a stable cell line in the presence of Cdk5/p35. Upon phosphatase treatment, the pCaV2.2 signal was abolished.

(C) After immunoprecipitation with anti-CaV2.2 antibody, the pCaV2.2 antibody was used to probe for phosphorylated N-type calcium channel signal. In the Cdk5 cKO brain lysates, phosphorylation was significantly decreased, indicating that the S2013 site of CaV2.2 is indeed an in vivo Cdk5 substrate. Right: Quantification of phosphorylation levels in Cdk5 cKO brain lysates. Normalized protein levels are shown, with n = 3 per condition. Control, 1.00 ± 0.14; Cdk5 cKO, 0.35 ± 0.02; **$p < 0.01$.

Data are shown as the mean ± SEM. Statistical significance was calculated using Student's t test (*$p < 0.05$; **$p < 0.01$; ***$p < 0.001$). See also Figure S2.

phosphorylation of CaV2.2 increased the channel open probability, P_o (Figures 4E and 4F). Importantly, the Cdk5/p35-mediated increase in the WT CaV2.2 channel open probability was not observed in 8X CaV2.2.

To further determine whether the dramatic increase in CaV2.2 current density impacts CaV2.2 surface expression in primary neurons, we cloned the full-length WT CaV2.2 α_1 subunit or the 8X CaV2.2 α_1 subunit cDNA into a bicistronic herpes simplex virus (HSV) backbone that coexpresses green fluorescent protein (GFP) (Neve et al., 2005). In primary neurons, transduction with HSV yields about 90% GFP-positive cells after 24 hr (Figure S4A). Upon transduction of primary neurons with WT CaV2.2 or 8X CaV2.2 HSV, however, there were no alterations in CaV2.2 surface levels compared to neurons transduced with control GFP HSV (Figure S4B). Collectively, these data suggest that in addition to increased channel availability, Cdk5-mediated phosphorylation of CaV2.2 results in increased calcium influx due to enhanced channel open probability.

Altered Synaptic Properties in Neurons Expressing CaV2.2

We predicted that Cdk5-mediated phosphorylation of CaV2.2 might play an important physiological role in CaV2.2-mediated neurotransmission. To test this hypothesis, whole-cell CaV2.2 currents were isolated in neurons transduced with HSV expressing control GFP, WT CaV2.2, or 8X CaV2.2. Consistent with our heterologous cell data, Cdk5-mediated phosphorylation of WT CaV2.2, but not 8X CaV2.2, increased neuronal CaV2.2 current density when compared to neurons expressing control GFP HSV (Figure 5A; Table S4). Furthermore, inhibition of Cdk5 activity using a dominant-negative Cdk5 (DNK5) HSV further reduced CaV2.2 current density (Figure 5A), suggesting that

Cdk5 is the major kinase responsible for CaV2.2 phosphorylation and increased CaV2.2 current density. We also examined whether the P/Q-type calcium channel (CaV2.1), the other major presynaptic calcium channel in neurons, was affected by expression of WT CaV2.2 or 8X CaV2.2 HSV but found no differences in CaV2.1 current densities compared to those of neurons expressing GFP HSV (Figure S5; Table S5). CaV2.1 current density was also unaffected by the expression of DNK5 HSV (Figure S5).

We next measured miniature postsynaptic currents to determine whether Cdk5-mediated phosphorylation of CaV2.2 impacts neurotransmitter release. To obtain miniature excitatory and inhibitory postsynaptic currents (mEPSCs and mIPSCs), primary neurons at DIV13-15 were transduced with GFP, WT CaV2.2, or 8X CaV2.2 HSV, and recordings were conducted 24–48 hr later. In neurons expressing WT CaV2.2 HSV, compared to those expressing GFP HSV, we observed increased frequencies of both mEPSCs and mIPSCs, with no changes in current amplitude (Figures 5B and 5C). However, neither the miniature frequency nor the amplitude of neurons expressing 8X CaV2.2 HSV differed significantly from those of neurons expressing GFP HSV (Figures 5B and 5C). The increased frequency of the miniature currents strongly suggests that Cdk5-mediated phosphorylation of WT CaV2.2 modulates presynaptic function by enhancing vesicle release.

To explore the effects of expressing CaV2.2 in presynaptic terminals at a higher resolution, cultured neurons were transduced with HSV expressing GFP, WT CaV2.2, or 8X CaV2.2 and fixed for monolayer electron microscopy. Consistent with the notion that increased release probability is related to the size of the readily releasable vesicle pool (Dobrunz and Stevens, 1997; Murthy et al., 1997), we found that the number of docked vesicles in the readily releasable pool was greater in the presynaptic terminals of neurons transduced with WT CaV2.2, but not
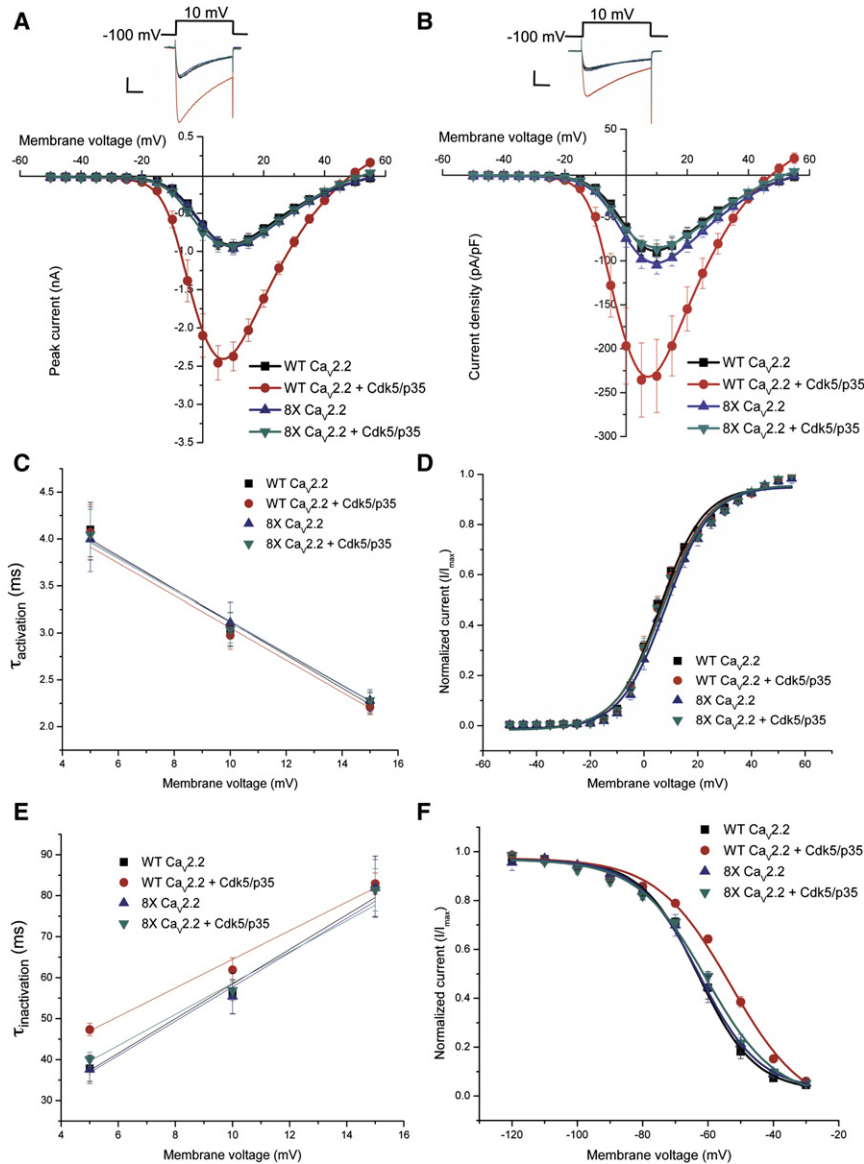
Figure 3. Modulation of Biophysical Properties of N-type Calcium Channels by Cdk5/p35

(A) Cdk5 dramatically increased N-type current amplitude in cells expressing WT $Ca_V2.2$. Inward currents were evoked by 100 ms step depolarizations applied to test potentials between −55 mV and +55 mV from a holding potential of −100 mV. Peak current amplitudes were plotted on a current-voltage (I/V) curve. While cells expressing 8X $Ca_V2.2$ passed inward current at similar levels to WT $Ca_V2.2$, the presence of Cdk5/p35 failed to increase N-type current in cells expressing 8X $Ca_V2.2$. Scale bars, 50 nA, 20 ms.

(B) Current density measurements were obtained by normalizing peak $Ca_V2.2$ current amplitude to cell capacitance. The current density of cells expressing WT $Ca_V2.2$ was significantly enhanced with coexpression of Cdk5/p35. Scale bars, 50 nA, 20 ms.

(C) A voltage-step protocol was applied and fitted an exponential curve to the time point spanning the maximal inward calcium current to obtain time constants for channel activation. Lines were plotted from best-fit linear regression. Cdk5/p35 phosphorylation of WT $Ca_V2.2$ did not affect activation kinetics at any of the membrane potentials tested (5 mV, 10 mV, 15 mV).

(D) Cdk5-mediated phosphorylation of $Ca_V2.2$ did not alter voltage dependence of activation. Cells were held at −100 mV, and tail currents from the test pulse were normalized to the largest tail current from each series. The normalized curves were fit by a single Boltzmann distribution $I/I_{max} = A2 + (A1 − A2)/(1 + exp((V_m − V_{1/2})/d_x))$, with $V_{1/2}$ as the midpoint for half-maximal activation, A1 and A2 being the normalized amplitudes and d_x the slope.

(E) A long voltage-step protocol was applied and fitted to an exponential curve to the time point at the peak inward current toward the end of the protocol to obtain inactivation time constants. Coexpression of Cdk5/p35 increased inactivation kinetics of WT $Ca_V2.2$ at the test potential of 5 mV.

(F) Cdk5-mediated phosphorylation of WT $Ca_V2.2$ affected the voltage-dependence of steady-state inactivation (SSI), a measure of the number of available channels at a given potential. Cells were held at −100 mV, and SSI values from the test pulse were normalized to the largest tail current. SSI curves were fitted by a single Boltzmann equation to calculate the membrane potential in which half of the channels are inactivated ($V_{1/2,inact}$). The rightward shift of the SSI curve indicated that coexpression of Cdk5/p35 augmented the number of WT $Ca_V2.2$ channels available for opening.

Data shown are the values (mean ± SEM) given in Table S1. Statistical significance was calculated by one-way ANOVA (Bonferroni multiple comparison test) (*$p < 0.05$; **$p < 0.01$; ***$p < 0.001$). See also Figure S3.

8X $Ca_V2.2$, HSV when compared to neurons transduced with GFP HSV (Figure 5D). These observations indicate that expression of WT $Ca_V2.2$ HSV in primary neurons facilitates neurotransmitter release due to an increased number of docked vesicles at the synaptic terminal.

In order to examine whether $Ca_V2.2$ localization itself might be affected by HSV expression, we performed immunocytochemistry and immunogold electron microscopy studies. Similar to previous reports (Maximov and Bezprozvanny, 2002), and consistent with the increased frequency of mEPSCs

and mIPSCs, expression of WT $Ca_V2.2$ HSV facilitated the synaptic localization of $Ca_V2.2$ (Figure 5E).While immunogold-labeled $Ca_V2.2$ was associated with the presynaptic terminal in neurons expressing GFP HSV, neurons transduced with WT $Ca_V2.2$ HSV displayed higher colocalization of $Ca_V2.2$ to the presynaptic area (Figure 5F). The localization effects were not observed in neurons transduced with 8X $Ca_V2.2$ HSV, which displayed a similar profile to neurons expressing GFP HSV. Therefore, Cdk5-mediated phosphorylation of WT $Ca_V2.2$ HSV facilitates neurotransmitter release by affecting the number of
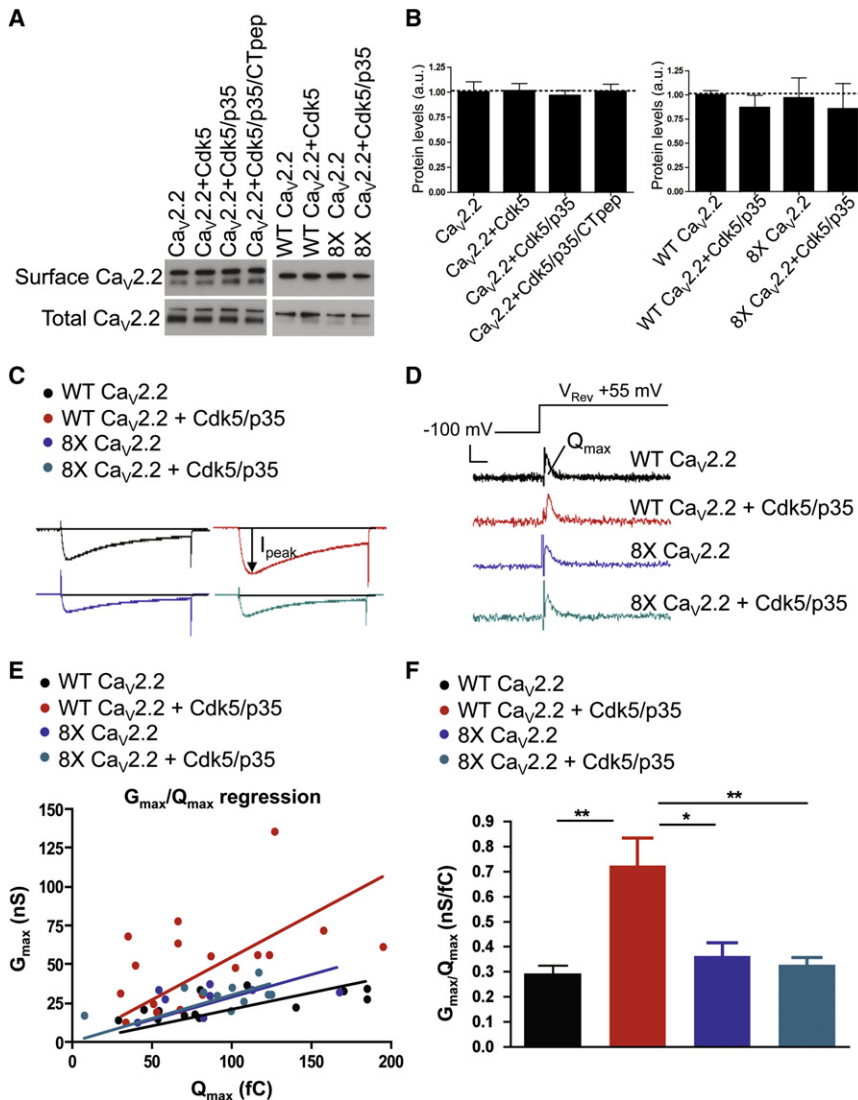
Figure 4. Analysis of Surface Expression Levels and Channel Open Probability after Cdk5-Mediated Phosphorylation of $Ca_V2.2$

(A) $Ca_V2.2$ surface expression levels were not altered by Cdk5-mediated phosphorylation. Left: In the stable cell line expressing $Ca_V2.2$, $Ca_V2.2$ was coexpressed with Cdk5 alone, Cdk5/p35, or Cdk5/p35 and a competing C-terminal peptide. Right: Compared to expression of WT $Ca_V2.2$ alone, surface levels of $Ca_V2.2$ protein were unaltered after WT $Ca_V2.2$ coexpression with Cdk5/p35, 8X $Ca_V2.2$ expression, or 8X $Ca_V2.2$ coexpression with Cdk5/p35.

(B) Quantification was performed across independent experiments. Normalized protein levels are shown, with n = 3 experiments per condition.

(C) Representative traces shown for peak current as a function of test-pulse potential. The I_{peak} was calculated by dividing the peak current by the cell capacitance to obtain maximal current.

(D) Transient currents occur when the cell is brought from its resting potential to the reversal potential (approximately +55 mV). The area under the transient current was calculated as Q_{max}. Scale bars, 0.1 nA, 2 ms.

(E) G_{max} (slope of the maximal current) was plotted against Q_{max}, with the ratio established as a measurement of the channel open probability.

(F) Quantification of G_{max}/Q_{max}. Cdk5-mediated phosphorylation of WT $Ca_V2.2$ increased channel open probability (P_o).

Data shown are the values (mean ± SEM) given in Table S3. Statistical significance was calculated using a one-way ANOVA (Tukey's multiple comparison test) (*$p < 0.05$; **$p < 0.01$; ***$p < 0.001$). See also Figure S4.

docked vesicles and also by increasing $Ca_V2.2$ localization at the synapse.

Interactions between $Ca_V2.2$ and Active-Zone Proteins Are Affected by Cdk5

To gain additional insight into the molecular mechanisms underlying the effects of Cdk5-mediated N-type calcium channel phosphorylation on neurotransmitter release, we transduced primary hippocampal neurons at DIV13-15 with GFP, WT $Ca_V2.2$, or 8X $Ca_V2.2$ HSV. The associations between $Ca_V2.2$ and various presynaptic proteins involved in synaptic vesicle scaffolding or fusion were then examined using coimmunoprecipitation and immunoblotting after 24–48 hr in vitro. While the overall protein levels of multiple presynaptic components were unaltered, the binding of $Ca_V2.2$ to the active-zone protein RIM1 was significantly increased in neurons transduced with WT $Ca_V2.2$ HSV compared to neurons transduced with GFP HSV (Figure 6A; Table S6). Since RIM1 directly binds and tethers

both $Ca_V2.1$ (P/Q-type) and $Ca_V2.2$ (N-type) channels to the synaptic cleft to facilitate synchronous neurotransmitter release (Kaeser et al., 2011), these results indicate that Cdk5-mediated phosphorylation of $Ca_V2.2$ may play a role in modulating $Ca_V2.2$ and RIM1 binding, thereby affecting vesicle docking and neurotransmitter release. We found that acute inhibition of Cdk5 by DNK5 HSV in primary neurons reduced the association between $Ca_V2.2$ and RIM1, providing further support that Cdk5-mediated phosphorylation of $Ca_V2.2$ regulates its association with RIM1 (Figure S6A; Table S7). Furthermore, in brain lysates from control and Cdk5 cKO mice, chronic Cdk5 depletion reduced the binding of $Ca_V2.2$ to RIM1, indicating that Cdk5 is necessary for maintaining the association between $Ca_V2.2$ and RIM1 (Figure 6B). We observed that $Ca_V2.2$ binding to Syntaxin1A in Cdk5 cKO lysates was also reduced. These data demonstrate that Cdk5-mediated phosphorylation of $Ca_V2.2$ is required for its interaction with RIM1 and other SNARE proteins.

$Ca_V2.2$ Phosphorylation by Cdk5 Affects Basal Synaptic Transmission and Alters Paired-Pulse Facilitation

Because Cdk5-mediated phosphorylation of $Ca_V2.2$ enhances miniature excitatory and inhibitory postsynaptic currents by

modulating presynaptic release probability, we reasoned that synaptic plasticity would also be affected. To address this hypothesis, we performed stereotaxic delivery of GFP, WT Ca$_V$2.2, or 8X Ca$_V$2.2 HSV into hippocampal area CA3 (Figure S6B). In an additional set of experiments, WT Ca$_V$2.2 or 8X Ca$_V$2.2 HSV was coinjected with DNK5 HSV, and the results were compared to those from injection of WT Ca$_V$2.2 or 8X Ca$_V$2.2 HSV alone. Acute transverse hippocampal slices were prepared to assess various forms of synaptic plasticity at days 2–3 postinjection. A concentric bipolar electrode was placed in the stratum radiatum to stimulate the Schaffer collateral/ commissural pathway fibers, and field recordings were obtained from the dendritic region of hippocampal area CA1.

We first obtained input-output curves, and in contrast to slices expressing control GFP HSV, we discovered a significant enhancement of basal synaptic transmission in slices transduced with WT Ca$_V$2.2 HSV. This enhancement of basal synaptic transmission was not present in slices expressing 8X Ca$_V$2.2 HSV (Figure 7A; Table S8). Furthermore, the enhanced basal synaptic transmission observed in slices expressing WT Ca$_V$2.2 HSV alone was abolished in the presence of DNK5 HSV (Figure S7A; Table S9). We next examined paired-pulse facilitation (PPF), a form of short-term synaptic plasticity that predicts release probability (Zucker and Regehr, 2002). Strikingly, the PPF ratios calculated at multiple intervals were significantly lower in slices expressing WT Ca$_V$2.2 HSV than in those expressing GFP HSV. The PPF ratios were not significantly different between slices expressing GFP HSV and 8X Ca$_V$2.2 HSV (Figure 7B). However, the reduction in PPF ratio observed in slices expressing WT Ca$_V$2.2 HSV alone was absent in slices coexpressing WT Ca$_V$2.2 and DNK5 HSV (Figure S7B). The results are consistent with the hypothesis that neurons transduced with WT Ca$_V$2.2 HSV have a higher release probability and indicate that the enhancement of synaptic transmission relies on the activity of Cdk5.

Cdk5-Mediated Phosphorylation of N-type Calcium Channels Impacts Presynaptic Plasticity

To explore whether Cdk5-mediated phosphorylation of Ca$_V$2.2 affects synaptic facilitation, another form of presynaptic plasticity, we applied different stimulus trains to the Schaffer collateral pathway. Synaptic facilitation did not differ between slices expressing GFP and 8X Ca$_V$2.2 HSV. As predicted for neurons with lower PPF, and therefore higher release probability, slices expressing WT Ca$_V$2.2 HSV exhibited a reduction in transient facilitation elicited during the stimulation (100 Hz at 0.5 mM [Ca^{2+}]$_o$) (Figure 7C). Moreover, the facilitation in slices expressing WT Ca$_V$2.2 HSV alone was absent when DNK5 HSV was coexpressed with WT Ca$_V$2.2 HSV, demonstrating the requirement of Cdk5 activity for Ca$_V$2.2-mediated synaptic facilitation (Figure S7C).

We next examined short-term synaptic plasticity elicited by high-frequency stimuli (HFS). Compared to slices transduced with GFP HSV, there was a strong reduction in the initial field excitatory postsynaptic potential (fEPSP) slope following HFS in slices transduced with WT Ca$_V$2.2 HSV (Figure 7D). There were no differences in initial fEPSP slope between slices expressing GFP and 8X Ca$_V$2.2 HSV. Early-phase long-term potentiation (LTP), measured at 30 min poststimulation, was also

considerably reduced in slices expressing WT Ca$_V$2.2 HSV when compared to slices expressing GFP HSV (Figure 7D). However, the altered plasticity in slices expressing WT Ca$_V$2.2 HSV alone was not observed with coexpression of DNK5 HSV (Figure S7D). In all experiments, there were no significant differences in plasticity measurements between slices expressing 8X Ca$_V$2.2 HSV alone and slices coexpressing 8X Ca$_V$2.2 and DNK5 HSV (Figures S7A–S7D). Collectively, these results demonstrate that Cdk5-mediated phosphorylation of WT Ca$_V$2.2 increases basal synaptic transmission and enhances presynaptic release probability, which in turn decreases synaptic facilitation and early-phase LTP.

DISCUSSION

Here we demonstrated that the N-type calcium channel is a Cdk5 substrate. Phosphorylation of Ca$_V$2.2 by Cdk5 significantly increased calcium-current density and channel open probability. We further showed that the interaction between Ca$_V$2.2 and RIM1 was modulated by Cdk5, which provided a molecular mechanism for the increased number of docked vesicles at the presynaptic terminal in neurons expressing Ca$_V$2.2. We also found presynaptic alterations in plasticity associated with Cdk5-mediated phosphorylation of Ca$_V$2.2 that included enhanced basal synaptic transmission, enhanced presynaptic release probability, and an overall reduction in short-term facilitation. Importantly, these effects were not observed with the Cdk5 phosphorylation mutant 8X Ca$_V$2.2, either alone or in the presence of Cdk5. Taken together, these studies demonstrate a pivotal role for Cdk5-mediated posttranslational modifications of the N-type calcium channel in regulating presynaptic function, and they highlight the close interaction between kinases and calcium channels in neurons.

Protein Kinases that Impact Calcium Channel Function

While this study shows that Ca$_V$2.2 is a Cdk5 substrate, previous work has implicated several kinases in the modulation of voltage-gated calcium channels (Bannister et al., 2005). The calcium-calmodulin kinase II (CaMKII) interacts with the P/Q-type calcium channel to facilitate transmitter release (Jiang et al., 2008), and the glycogen synthase kinase (GSK3β) phosphorylates the P/Q-type calcium channel in the intracellular II-III loop (Zhu et al., 2010) to inhibit vesicle exocytosis by disrupting SNARE complex formation. Other kinases that target Ca$_V$2.2 include protein kinases A and C (PKA and PKC), and both PKA- and PKC-mediated phosphorylation of Ca$_V$2.2 inhibit Ca$_V$2.2 interaction with SNARE complexes (Yokoyama et al., 1997). PKC-mediated phosphorylation of Ca$_V$2.2 also enhances N-type calcium current by reducing the G-protein inhibition of Ca$_V$2.2 (Swartz et al., 1993). Furthermore, PKC phosphorylation of Ca$_V$2.2 in the I-II linker region reduces the inhibitory effect of the Gβγ subunits on Ca$_V$2.2 (Zamponi et al., 1997). Notably, the Ca$_V$2.2 N-terminus, together with the I-II region, plays a fundamental role in modulating Gβγ inhibition (Agler et al., 2005). Altogether, these results provide a complex representation of signaling pathways involving kinases, second messengers such as Gβγ subunits, and synaptic release machinery such as SNARE proteins leading up to neurotransmitter release.
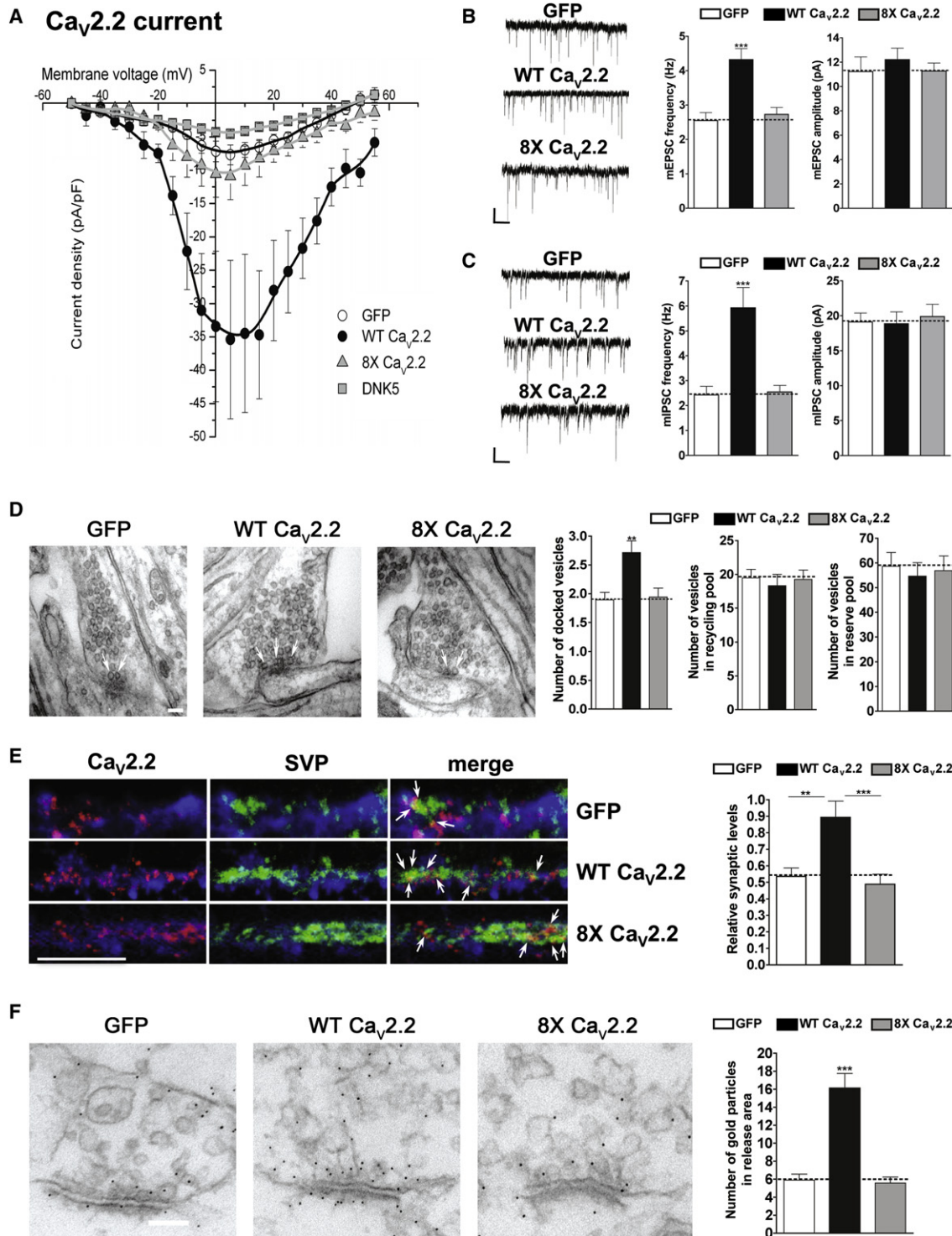
Figure 5. Neurotransmitter Release Impacted by Cdk5-Mediated Phosphorylation of Ca$_V$2.2

(A) Current-voltage relationship of neurons expressing GFP, WT Ca$_V$2.2, 8X Ca$_V$2.2, or DNK5 HSV. Compared to Ca$_V$2.2-mediated current density in neurons expressing GFP, Cdk5-mediated phosphorylation of WT Ca$_V$2.2, but not 8X Ca$_V$2.2, enhanced Ca$_V$2.2 current density. However, expression of DNK5 HSV further reduced Ca$_V$2.2 current.

(B) Sample traces (left) and quantification (right) of the frequency and amplitude of the miniature excitatory postsynaptic currents (mEPSCs). Compared to neurons expressing GFP HSV, the frequency of mEPSCs was increased in hippocampal neurons expressing WT Ca$_V$2.2 HSV. There were no significant differences in mEPSC amplitudes. Scale bars, 10 pA, 2 s.

Pharmacological inhibition of Cdk5 using roscovitine was previously used to examine calcium channel function (Tomizawa et al., 2002). However, in addition to inhibiting Cdk5, roscovitine is an inhibitor of cyclin-dependent kinases 1, 2, 5, and 7 (Bach et al., 2005) and also acts directly on calcium channels by binding to the extracellular domain of L-type calcium channels (Yarotskyy and Elmslie, 2007). Furthermore, extracellular roscovitine application potentiates (P/Q-type) Ca$_V$2.1-mediated neurotransmitter release to slow deactivation kinetics (Yan et al., 2002) and increase the inactivation of Ca$_V$2.2 (Buraei et al., 2005). This may account for the differences observed between our study and a previous study demonstrating fEPSP enhancement following roscovitine application on hippocampal slices, which preferentially affected P/Q-type calcium channels (Tomizawa et al., 2002). Therefore, in our efforts to understand how Ca$_V$2.2 is regulated at the presynaptic terminal, we examined the regulation of Ca$_V$2.2 in the context of endogenous Cdk5 activity in neurons and inhibited Cdk5 with a dominant-negative Cdk5 virus rather than using roscovitine.

Regulation of Protein-Protein Interactions and Presynaptic Plasticity by Cdk5

Our findings also revealed a role for Cdk5-mediated phosphorylation of Ca$_V$2.2 in modulating the interactions of Ca$_V$2.2 with various active-zone proteins, including RIM1, to regulate neurotransmission and presynaptic plasticity. It was previously reported that RIM1 binds the auxiliary β subunit of both N-type and P/Q-type calcium channels to facilitate calcium influx and tether vesicles to the presynaptic terminal (Kiyonaka et al., 2007). Intriguingly, RIM1 also further reduces the G-protein-mediated inhibition of Ca$_V$2.2, which subsequently contributes to a prolonged increase in calcium influx (Weiss et al., 2011). As RIM1 is required for calcium-channel density and vesicle docking at the active zone of calyx of Held synapses and central synapses (Han et al., 2011; Kaeser et al., 2011), our results are consistent with the notion that the Ca$_V$2.2 interaction with RIM1 allows for coordinated transmitter release, and we propose that this interaction is regulated in part by Cdk5-mediated phosphorylation of Ca$_V$2.2.

Ca$_V$2.2 and RIM1 are both closely associated with other active-zone proteins and SNARE complexes. In this study, we examined the binding of Ca$_V$2.2 to a number of presynaptic proteins, and showed that RIM binding increased in neurons expressing WT Ca$_V$2.2 HSV. Several groups previously reported a direct interaction between RIM1, or the RIM1 binding protein (RIMBP), and Ca$_V$2.2 (Coppola et al., 2001; Hibino et al., 2002; Kaeser et al., 2011). However, our results differ from other reports that RIM1 does not bind Ca$_V$2.2, even though both localize to the presynaptic terminal (Khanna et al., 2006, 2007b). A possible explanation might be the previous use of an antibody targeting the synprint region of chicken Ca$_V$2.2 (Li et al., 2004), even though one study was conducted on rat brain preparations (Khanna et al., 2007a). The chicken synprint region shares only about 59% homology to the mouse and rat synprint regions, which share 88% homology with each other. Therefore, the different antibodies that were used might explain the discrepancies between our findings and those published previously.

Although we did not observe a decrease in Ca$_V$2.2 binding to Syntaxin1A in primary neurons, in contrast to our Cdk5 cKO samples, we hypothesize that acute manipulations differ from chronic Cdk5 knockdown in vivo, which may in turn directly or indirectly affect the interaction of Ca$_V$2.2 with various SNARE proteins to alter neurotransmission. We also cannot exclude the possibility that other kinases, such as PKA, may phosphorylate Ca$_V$2.2 at similar residues and promote similar functions. It is also possible that the β or α2δ auxiliary subunits, which also modulate calcium channel function and have previously been shown to be regulated by phosphorylation (Viard et al., 2004), are additional Cdk5 substrates that can modify Ca$_V$2.2 and SNARE protein interactions.

We demonstrated that Cdk5 impacts Ca$_V$2.2 channel availability and channel open probability. It will be intriguing to further elucidate how Cdk5-mediated phosphorylation of Ca$_V$2.2 may result in conformational alterations between the α$_1$ subunit and other channel subunits, or potentially with the pore-forming domain, to influence channel gating properties. In line with previous reports, overexpression of Ca$_V$2.2 did not affect the Ca$_V$2.1 (P/Q-type calcium channel) current (Cao and Tsien, 2010). However, in our study, acute slices expressing WT Ca$_V$2.2 HSV exhibited decreased PPF, which is in agreement with some previous findings (Ahmed and Siegelbaum, 2009) but in contrast to others, in which no alterations in PPF were observed (Cao and Tsien, 2010). This may be due to differences in Schaffer collateral field recordings versus single-cell recordings of dissociated hippocampal neurons. Thus, in future studies

---

(C) Sample traces (left) and quantification (right) of the frequency and amplitude of the miniature inhibitory postsynaptic currents (mIPSCs). Compared to neurons expressing GFP HSV, the frequency of mIPSCs was increased in hippocampal neurons expressing WT Ca$_V$2.2 HSV. There were no significant differences in mIPSC amplitudes. Scale bars, 10 pA, 2 s.

(D) Electron microscopy images from neurons transduced with GFP, WT Ca$_V$2.2, or 8X Ca$_V$2.2 HSV. Scale bar, 100 nm. Compared to neurons expressing GFP HSV, there was an increase in the number of docked vesicles in the presynaptic terminal of neurons expressing WT Ca$_V$2.2 HSV. There were no significant differences in vesicle properties of neurons expressing 8X Ca$_V$2.2 HSV when compared to neurons expressing GFP HSV.

(E) Approximately five to seven HSV-transduced neurons (GFP-positive cells from HSV transduction; blue) per culture in three independent experiments were used to quantify the relative synaptic localization of Ca$_V$2.2 (red) by assessing its colocalization with presynaptic marker Synaptophysin (green). Compared to neurons expressing GFP HSV, expression of WT Ca$_V$2.2 HSV increased the synaptic colocalization of Ca$_V$2.2 and Synaptophysin. Right: quantification of synaptic levels. Scale bar, 5 μm.

(F) Immunogold labeling for primary hippocampal neurons at DIV16 transduced with GFP, WT Ca$_V$2.2, or 8X Ca$_V$2.2 HSV. There was increased Ca$_V$2.2 localization to the presynaptic terminal in neurons expressing WT Ca$_V$2.2 HSV when compared to neurons expressing GFP HSV. Scale bar, 100 nm. Right: quantification of the immunogold labeling.

Data shown are the values (mean ± SEM) given in Table S4. Statistical significance was calculated using a one-way ANOVA (Tukey's multiple comparison test). (*p < 0.05; **p < 0.01; ***p < 0.001).
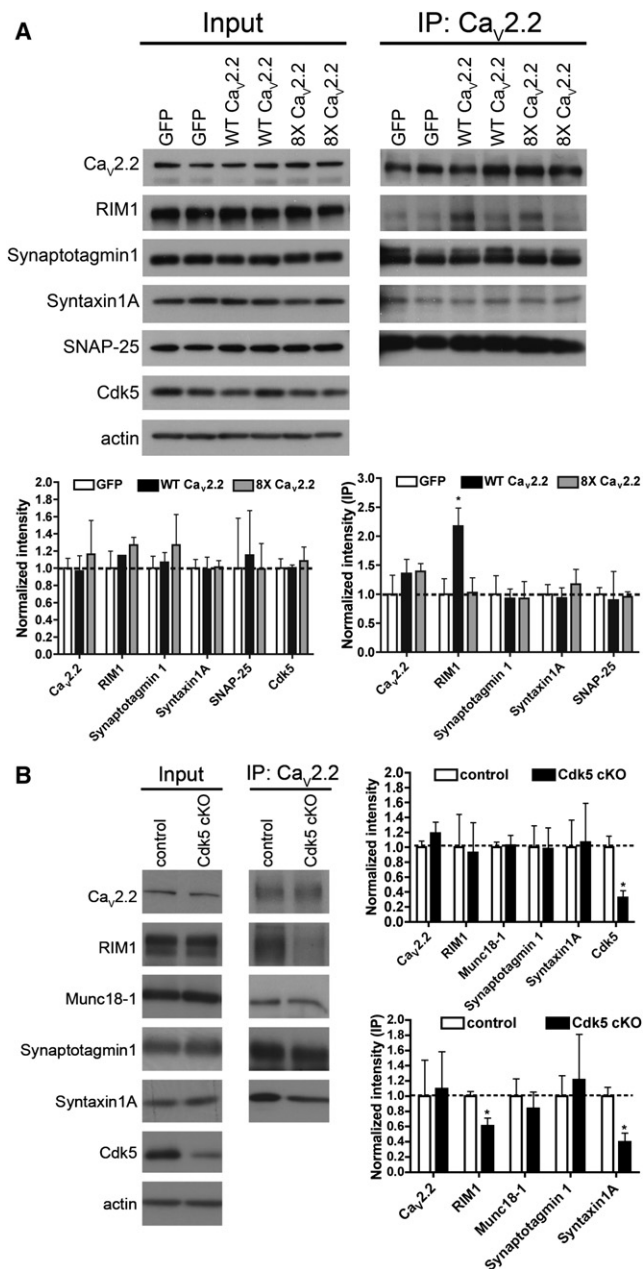
Figure 6. Interactions between Ca$_V$2.2 and Active-Zone Proteins Are Affected by Cdk5

(A) Presynaptic proteins were probed in neurons transduced with GFP, WT Ca$_V$2.2, or 8X Ca$_V$2.2 HSV. Immunoprecipitation with Ca$_V$2.2 revealed an increase in the association between Ca$_V$2.2 and RIM1 in neurons expressing WT Ca$_V$2.2 HSV relative to neurons expressing GFP HSV.

(B) Chronic Cdk5 depletion reduced the association between Ca$_V$2.2 and RIM1. The interaction between Ca$_V$2.2 and Syntaxin1A was also reduced. Normalized protein levels are shown, with n = 3 mice per condition.

Data shown are the values (mean ± SEM) given in Table S6. Statistical significance was calculated using a one-way ANOVA (Tukey's multiple comparison test, Bonferroni multiple comparison test) or Student's t test ($*p < 0.05$; $**p < 0.01$; $***p < 0.001$).

it will be important to further probe how Cdk5-mediated phosphorylation of Ca$_V$2.2 affects its contribution to excitatory postsynaptic currents. As Cdk5 and Ca$_V$2.2 are present in GABAergic interneurons (Poncer et al., 1997; Rakić et al., 2009), it would also be interesting to determine whether Cdk5 differentially affects excitatory and inhibitory neurotransmission.

The Role of Cdk5 in Homeostatic Mechanisms

Combined with those of previous studies, our data suggest that both Ca$_V$2.2 and Cdk5 mediate presynaptic plasticity by regulating neurotransmitter release. Recent literature suggests that Cdk5 is a central regulator of synaptic homeostasis. Cdk5 activity is required for the downregulation of heightened synaptic activity via phosphorylation of the postsynaptic protein SPAR. This priming effect allows Polo-like kinase 2 to promote the degradation of SPAR during homeostatic scaling (Seeburg et al., 2008). Cdk5 also serves as a control point for neurotransmission, as inhibition of Cdk5 activity by roscovitine results in access to the resting synaptic vesicle pool (Kim and Ryan, 2010). Furthermore, Cdk5 activity is critical for the presynaptic adaptation of hippocampal CA3 recurrent circuitry under chronic inactivity, as it mediates reduced connectivity after silencing synapses but enhances synaptic strength of the remaining connections (Mitra et al., 2011). Precisely how levels of Cdk5, and Cdk5/p35 activity, are regulated under physiological or excitotoxic conditions to impart its action on Ca$_V$2.2 in specific cell populations remains an exciting topic for future work, which may also reveal additional Ca$_V$2.2 binding partners, as well as Cdk5 substrates that play a vital role in synaptic homeostasis.

In summary, our data demonstrate a previously uncharacterized interaction between Ca$_V$2.2 and Cdk5 that results in a Cdk5-mediated increase in Ca$_V$2.2 current density, channel open probability, and altered Ca$_V$2.2 interaction with the active-zone protein RIM1 to ultimately affect neurotransmission and plasticity by promoting vesicle docking and release. These findings provide a framework to examine how Ca$_V$2.2 is regulated in the context of endogenous Cdk5 activity. Given the significant implications of Cdk5 in synaptic homeostasis, a compelling question is how posttranslational modifications of Ca$_V$2.2 impact its interactions with other key presynaptic proteins involved in vesicle docking, neurotransmission, and plasticity.

EXPERIMENTAL PROCEDURES

In Vitro Kinase Assay

GST vector alone or various GST-Ca$_V$2.2 intracellular fusion protein fragments were purified and incubated with purified p25/Cdk5 kinase (Cell Signaling Technology) in kinase buffer for 30 min at room temperature. The reaction was stopped with the addition of 2X sample buffer, separated by 10% SDS-PAGE polyacrylamide gels (Bio-Rad), stained with Coomassie blue (SimplyBlue Safestain, Invitrogen) and then dried prior to analysis by autoradiography.

Antibodies

To generate the phosphospecific antibody to S2013 in rat Ca$_V$2.2, a 13-amino-acid phosphorylated and nonphosphorylated peptide, NH2-QPAPNASPMKRSC-COOH, was synthesized and purified using high-performance liquid chromatography (Tufts Core Facility, Physiology Dept). The peptides were conjugated to KLH for polyclonal rabbit antibody production (Covance Research Products). Antisera were affinity purified and collected
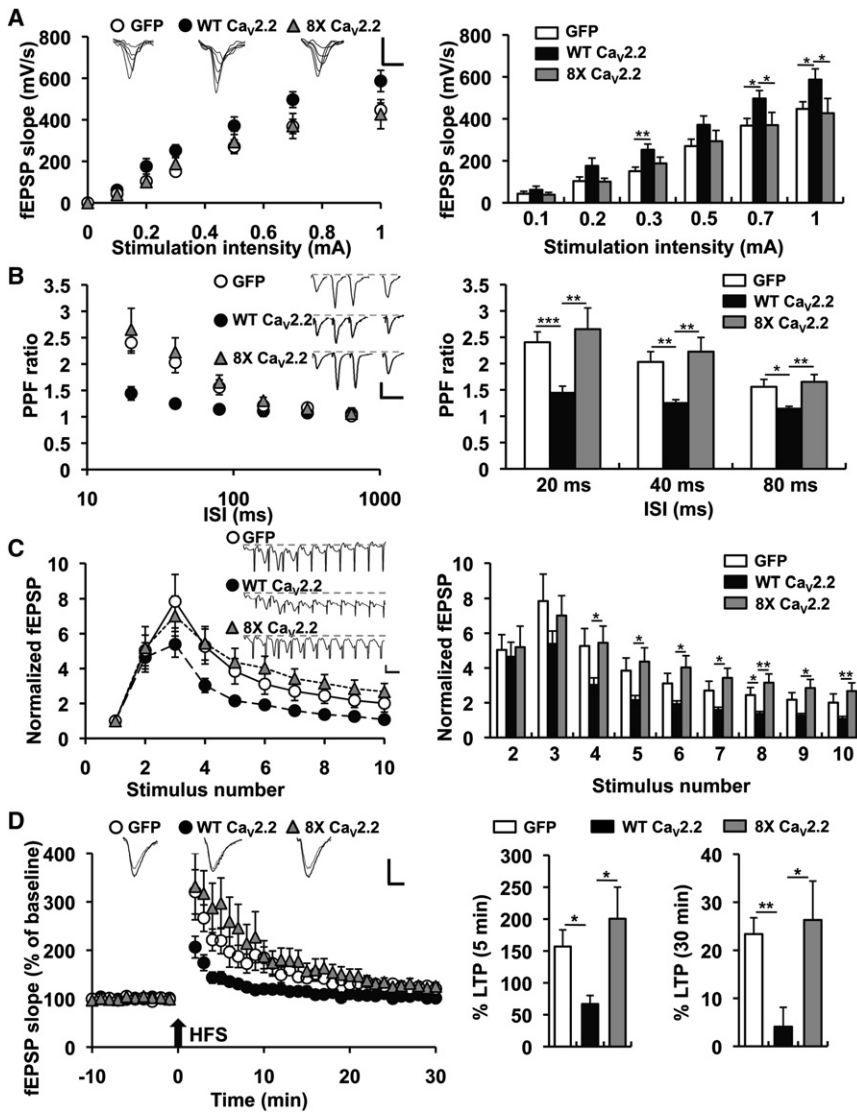
Figure 7. Synaptic Plasticity Measurements after Expression of Ca$_V$2.2 HSV in Hippocampus

(A) Representative traces and quantification of the input/output curve in acute hippocampal slices transduced in area CA3 with GFP, WT Ca$_V$2.2, or 8X Ca$_V$2.2 HSV. Compared to slices expressing control GFP HSV, slices expressing WT Ca$_V$2.2 HSV exhibited enhanced basal synaptic transmission in the Schaffer collateral pathway. Scale bars, 0.5 mV, 10 ms. Right: quantification of the input/output curve.

(B) Representative traces and quantification of the paired-pulse facilitation (PPF) response in acute hippocampal slices transduced in area CA3 with GFP, WT Ca$_V$2.2, or 8X Ca$_V$2.2 HSV. Scale bars, 0.5 mV, 25 ms. Compared to slices expressing GFP HSV, slices expressing WT Ca$_V$2.2 exhibited significantly lower PPF ratios. Scale bars, 0.5 mV, 25 ms. Right: quantification of the PPF ratio at various stimuli.

(C) Representative traces and quantification of short-term facilitation during the 100 Hz stimulus at 0.5 mM [Ca^{2+}]$_o$. Slices expressing WT Ca$_V$2.2 HSV exhibited an overall reduction in synaptic facilitation during the 100 Hz stimulus train when compared to slices expressing GFP HSV. Scale bars, 0.5 mV, 10 ms. Right: quantification of the short-term plasticity at various stimuli.

(D) Representative traces and quantification before and after HFS induction. Compared to hippocampal slices expressing GFP HSV, the fEPSP slope was markedly decreased in slices expressing WT Ca$_V$2.2 HSV. In all plasticity measurements, there were no significant differences in synaptic properties between slices expressing GFP HSV alone and 8X Ca$_V$2.2 HSV. Scale bars, 0.5 mV, 10 ms. Right: quantification of the fEPSP slope immediately after HFS (5 min) and at the end of the 30 min period.

Data shown are the values (mean ± SEM) given in Table S8. Statistical significance was calculated using a one-way ANOVA (t test) (*p < 0.05; **p < 0.01; ***p < 0.001).

after passing through non-phospho peptide columns using a SulfoLink immobilization kit for peptides (Thermo Scientific).

Expression Plasmids and Constructs

The vector pGEX-4T0-2 (GE Healthcare) was used for cloning the rat isoform of Ca$_V$2.2 into various GST-Ca$_V$2.2 fragments (accession number AF055477). Mutagenesis of the GST-Ca$_V$2.2 fragments or full-length human isoform of Ca$_V$2.2 (accession number NM_000718) was carried out as described using the outlined protocol (QuickChange, Stratagene) and sequence verified (MIT Biopolymer Facility, Cambridge). GST fusion proteins were then generated and purified according to standard techniques.

Primary Neurons

Primary hippocampal or cortical neurons were obtained from E15-17 timed-pregnant Swiss Webster mice (Taconic), dissected in Hank's balanced salt solution with 20 mM HEPES, and plated at a density of 50,000 cells/cm^2.

Electrophysiology

Confluent tSA-201 cells were transfected using Lipofectamine 2000 at a 1:2:1 ratio of the α$_{1B}$, β3, and α2$_b$δ subunits with either GFP or Cdk5/p35-GFP according to the protocol (Invitrogen). For whole-cell patch clamp recordings, electrodes were pulled to a resistance of 3–6 MΩ (Sutter Instruments) and fire-polished (Narishige Instruments). The external solution consisted of (in mM) 150 TEA-Cl, 5 BaCl$_2$, 1 MgCl$_2$, 10 glucose, 10 HEPES (pH 7.3) (TEAOH), osmolality 320 ± 5. The internal solution contained (in mM) 135 CsCl, 4 MgCl$_2$, 4 Mg-ATP, 10 HEPES, 10 EGTA, and 1 EDTA, adjusted to pH 7.2 with TEAOH, osmolality 300 ± 10. For whole-cell patch clamp recordings obtained from cultured hippocampal neurons at DIV12-15, cells were transduced with HSV for 1-2 days prior to recordings (Neve et al., 2005). The external medium was the same as above, except for TEA-Cl (140 mM) and BaCl$_2$ (10 mM), and was supplemented with 1 μM tetrodotoxin (TTX), 10 μM Nifedipine (Tocris), and 200 nM ω-agatoxin-TK (Peptides International) to isolate Ca$_V$2.2 currents, or 2 μM ω-conotoxin GVIA to isolate Ca$_V$2.1 currents.

For miniature recordings, the external solution consisted of (in mM) 140 NaCl, 4 KCl, 2 CaCl$_2$, 2 MgCl$_2$, 10 HEPES, and 10 glucose (pH 7.3 with NaOH), 315 mOsm. The internal solution contained (in mM) 145 CsCl, 5 NaCl, 10 HEPES, 10 EGTA, 4 Mg-ATP, and 0.3 Na$_2$-GTP (pH 7.3 with CsOH), 305 mOsm. The external solution also contained 1 μM TTX, 50 μM picrotoxin (PTX), and 50 μM D-APV for mEPSCs, or 1 μM TTX, 10 μM CNQX, and 50 μM D-APV for mIPSCs. Series resistance was compensated

by 70%–90% with a 10 μs lag, and online leak correction was performed with a P/-4 protocol. Recordings were obtained at room temperature using an inverted fluorescent microscope (Zeiss). Data were acquired using the Axopatch 200B amplifier and analyzed with the pClamp10 and Origin8 software (Molecular Devices).

For field excitatory postsynaptic potential (fEPSP) recordings, acute transverse hippocampal slices were prepared from mice transduced with GFP, WT Ca$_V$2.2 or 8X Ca$_V$2.2 HSV according to standard techniques. The brain was rapidly removed and transferred to a sucrose-based cutting solution, and hippocampal slices were obtained using a vibratome and placed in a chamber filled with ACSF for 1 hr prior to Schaffer collateral stimulation. Experiments were performed blind to the group of subjects. Sample traces represent fEPSPs at 1 min before (gray trace) and 30 min after (black trace) HFS. Bar graph: average slopes of fEPSP during the first 5 min after HFS or the last 5 min of recording (percentage of baseline response). Full details are available in the Supplemental Experimental Procedures.

Surface Biotinylation Assay
Surface biotinylation assay was conducted as essentially described according to the protocol (Thermo Scientific).

Biochemistry
Samples were lysed in RIPA buffer with protease and phosphatase inhibitors. Protein samples were quantified prior to immunoprecipitation and processed according to standard immunoblotting techniques.

Electron Microscopy
For electron microscopy experiments, DIV14-17 neurons were transduced with HSV containing either GFP, WT Ca$_V$2.2, or 8X Ca$_V$2.2 overnight. Cells were fixed, embedded, cut on a microtome, and picked up on copper grids.

Immunocytochemistry
Primary hippocampal neurons were fixed in 4% paraformaldehyde, permeabilized with Triton X-100, and blocked with BSA/PBS. After incubation with primary antibodies, coverslips were rinsed, incubated in secondary antibodies, and mounted for confocal microscopy.

Surgery and Viruses
Animals were group housed in the small animal facility at the Department of Brain and Cognitive Sciences of Massachusetts Institute of Technology (Cambridge, MA) and handled according to the protocols in accordance with the National Institute of Health Guide for the Care and Use of Laboratory Animals. Eight-week old C57Bl/6J male mice were used for bilateral stereotaxic injections into hippocampal area CA3 (Jackson Labs). Detailed methods can be found in the Supplemental Experimental Procedures.

SUPPLEMENTAL INFORMATION

Supplemental Information includes seven figures, nine tables, and Supplemental Experimental Procedures and can be found with this article online at http://dx.doi.org/10.1016/j.neuron.2012.06.023.

REFERENCES

Agler, H.L., Evans, J., Tay, L.H., Anderson, M.J., Colecraft, H.M., and Yue, D.T. (2005). G protein-gated inhibitory module of N-type (ca$_V$2.2) Ca^{2+} channels. Neuron 46, 891–904.

Ahmed, M.S., and Siegelbaum, S.A. (2009). Recruitment of N-Type Ca^{2+} channels during LTP enhances low release efficacy of hippocampal CA1 perforant path synapses. Neuron 63, 372–385.

Bach, S., Knockaert, M., Reinhardt, J., Lozach, O., Schmitt, S., Baratte, B., Koken, M., Coburn, S.P., Tang, L., Jiang, T., et al. (2005). Roscovitine targets, protein kinases and pyridoxal kinase. J. Biol. Chem. 280, 31208–31219.

Bannister, R.A., Mezu, U., and Adams, S. (2005). Phosphorylation-dependent regulation of voltage-gated Ca2+ channels. In Voltage-Gated Calcium Channels, Gerald Zamponi, ed. (New York: Kluwer Academic/Plenum Publishers), pp. 168–182.

Brittain, J.M., Piekarz, A.D., Wang, Y., Kondo, T., Cummins, T.R., and Khanna, R. (2009). An atypical role for collapsin response mediator protein 2 (CRMP-2) in neurotransmitter release via interaction with presynaptic voltage-gated calcium channels. J. Biol. Chem. 284, 31375–31390.

Buraei, Z., Anghelescu, M., and Elmslie, K.S. (2005). Slowed N-type calcium channel (Ca$_V$2.2) deactivation by the cyclin-dependent kinase inhibitor roscovitine. Biophys. J. 89, 1681–1691.

Cao, Y.Q., and Tsien, R.W. (2010). Different relationship of N- and P/Q-type Ca^{2+} channels to channel-interacting slots in controlling neurotransmission at cultured hippocampal synapses. J. Neurosci. 30, 4536–4546.

Catterall, W.A., and Few, A.P. (2008). Calcium channel regulation and presynaptic plasticity. Neuron 59, 882–901.

Chae, T., Kwon, Y.T., Bronson, R., Dikkes, P., Li, E., and Tsai, L.H. (1997). Mice lacking p35, a neuronal specific activator of Cdk5, display cortical lamination defects, seizures, and adult lethality. Neuron 18, 29–42.

Cheung, Z.H., Chin, W.H., Chen, Y., Ng, Y.P., and Ip, N.Y. (2007). Cdk5 is involved in BDNF-stimulated dendritic growth in hippocampal neurons. PLoS Biol. 5, e63.

Coppola, T., Magnin-Luthi, S., Perret-Menoud, V., Gattesco, S., Schiavo, G., and Regazzi, R. (2001). Direct interaction of the Rab3 effector RIM with Ca^{2+} channels, SNAP-25, and synaptotagmin. J. Biol. Chem. 276, 32756–32762.

Dobrunz, L.E., and Stevens, C.F. (1997). Heterogeneity of release probability, facilitation, and depletion at central synapses. Neuron 18, 995–1008.

Fu, W.Y., Chen, Y., Sahin, M., Zhao, X.S., Shi, L., Bikoff, J.B., Lai, K.O., Yung, W.H., Fu, A.K., Greenberg, M.E., and Ip, N.Y. (2007). Cdk5 regulates EphA4-mediated dendritic spine retraction through an ephexin1-dependent mechanism. Nat. Neurosci. 10, 67–76.

Guan, J.S., Su, S.C., Gao, J., Joseph, N., Xie, Z., Zhou, Y., Durak, O., Zhang, L., Zhu, J.J., Clauser, K.R., et al. (2011). Cdk5 is required for memory function and hippocampal plasticity via the cAMP signaling pathway. PLoS ONE 6, e25735.

Han, Y., Kaeser, P.S., Südhof, T.C., and Schneggenburger, R. (2011). RIM determines Ca^{2+} channel density and vesicle docking at the presynaptic active zone. Neuron 69, 304–316.

Hibino, H., Pironkova, R., Onwumere, O., Vologodskaia, M., Hudspeth, A.J., and Lesage, F. (2002). RIM binding proteins (RBPs) couple Rab3-interacting molecules (RIMs) to voltage-gated Ca^{2+} channels. Neuron 34, 411–423.

Jahn, R., Lang, T., and Südhof, T.C. (2003). Membrane fusion. Cell 112, 519–533.

Jiang, X., Lautermilch, N.J., Watari, H., Westenbroek, R.E., Scheuer, T., and Catterall, W.A. (2008). Modulation of Ca$_V$2.1 channels by Ca^{2+}/calmodulin-dependent protein kinase II bound to the C-terminal domain. Proc. Natl. Acad. Sci. USA 105, 341–346.

Kaeser, P.S., Deng, L., Wang, Y., Dulubova, I., Liu, X., Rizo, J., and Südhof, T.C. (2011). RIM proteins tether Ca²⁺ channels to presynaptic active zones via a direct PDZ-domain interaction. Cell *144*, 282–295.

Khanna, R., Li, Q., Sun, L., Collins, T.J., and Stanley, E.F. (2006). N type Ca²⁺ channels and RIM scaffold protein covary at the presynaptic transmitter release face but are components of independent protein complexes. Neuroscience *140*, 1201–1208.

Khanna, R., Li, Q., Bewersdorf, J., and Stanley, E.F. (2007a). The presynaptic Ca_V2.2 channel-transmitter release site core complex. Eur. J. Neurosci. *26*, 547–559.

Khanna, R., Zougman, A., and Stanley, E.F. (2007b). A proteomic screen for presynaptic terminal N-type calcium channel (Ca_V2.2) binding partners. J. Biochem. Mol. Biol. *40*, 302–314.

Kim, S.H., and Ryan, T.A. (2010). CDK5 serves as a major control point in neurotransmitter release. Neuron *67*, 797–809.

Kiyonaka, S., Wakamori, M., Miki, T., Uriu, Y., Nonaka, M., Bito, H., Beedle, A.M., Mori, E., Hara, Y., De Waard, M., et al. (2007). RIM1 confers sustained activity and neurotransmitter vesicle anchoring to presynaptic Ca²⁺ channels. Nat. Neurosci. *10*, 691–701.

Lai, M., Wang, F., Rohan, J.G., Maeno-Hikichi, Y., Chen, Y., Zhou, Y., Gao, G., Sather, W.A., and Zhang, J.F. (2005). A tctex1-Ca²⁺ channel complex for selective surface expression of Ca²⁺ channels in neurons. Nat. Neurosci. *8*, 435–442.

Lee, M.S., Kwon, Y.T., Li, M., Peng, J., Friedlander, R.M., and Tsai, L.H. (2000). Neurotoxicity induces cleavage of p35 to p25 by calpain. Nature *405*, 360–364.

Leenders, A.G., Lin, L., Huang, L.D., Gerwin, C., Lu, P.H., and Sheng, Z.H. (2008). The role of MAP1A light chain 2 in synaptic surface retention of Ca_V2.2 channels in hippocampal neurons. J. Neurosci. *28*, 11333–11346.

Li, Q., Lau, A., Morris, T.J., Guo, L., Fordyce, C.B., and Stanley, E.F. (2004). A syntaxin 1, Gα(o), and N-type calcium channel complex at a presynaptic nerve terminal: analysis by quantitative immunocolocalization. J. Neurosci. *24*, 4070–4081.

Lin, Y., McDonough, S.I., and Lipscombe, D. (2004). Alternative splicing in the voltage-sensing region of N-Type Ca_V2.2 channels modulates channel kinetics. J. Neurophysiol. *92*, 2820–2830.

Luebke, J.I., Dunlap, K., and Turner, T.J. (1993). Multiple calcium channel types control glutamatergic synaptic transmission in the hippocampus. Neuron *11*, 895–902.

Maximov, A., and Bezprozvanny, I. (2002). Synaptic targeting of N-type calcium channels in hippocampal neurons. J. Neurosci. *22*, 6939–6952.

Mitra, A., Mitra, S.S., and Tsien, R.W. (2011). Heterogeneous reallocation of presynaptic efficacy in recurrent excitatory circuits adapting to inactivity. Nat. Neurosci. *15*, 250–257.

Murthy, V.N., Sejnowski, T.J., and Stevens, C.F. (1997). Heterogeneous release properties of visualized individual hippocampal synapses. Neuron *18*, 599–612.

Neve, R.L., Neve, K.A., Nestler, E.J., and Carlezon, W.A., Jr. (2005). Use of herpes virus amplicon vectors to study brain disorders. Biotechniques *39*, 381–391.

Ohshima, T., Ward, J.M., Huh, C.G., Longenecker, G., Veeranna, Pant, H.C., Brady, R.O., Martin, L.J., and Kulkarni, A.B. (1996). Targeted disruption of the cyclin-dependent kinase 5 gene results in abnormal corticogenesis, neuronal pathology and perinatal death. Proc. Natl. Acad. Sci. USA *93*, 11173–11178.

Patrick, G.N., Zukerberg, L., Nikolic, M., de la Monte, S., Dikkes, P., and Tsai, L.H. (1999). Conversion of p35 to p25 deregulates Cdk5 activity and promotes neurodegeneration. Nature *402*, 615–622.

Poncer, J.C., McKinney, R.A., Gähwiler, B.H., and Thompson, S.M. (1997). Either N- or P-type calcium channels mediate GABA release at distinct hippocampal inhibitory synapses. Neuron *18*, 463–472.

Rakić, S., Yanagawa, Y., Obata, K., Faux, C., Parnavelas, J.G., and Nikolić, M. (2009). Cortical interneurons require p35/Cdk5 for their migration and laminar organization. Cereb. Cortex *19*, 1857–1869.

Samuels, B.A., Hsueh, Y.P., Shu, T., Liang, H., Tseng, H.C., Hong, C.J., Su, S.C., Volker, J., Neve, R.L., Yue, D.T., and Tsai, L.H. (2007). Cdk5 promotes synaptogenesis by regulating the subcellular distribution of the MAGUK family member CASK. Neuron *56*, 823–837.

Seeburg, D.P., Feliu-Mojer, M., Gaiottino, J., Pak, D.T., and Sheng, M. (2008). Critical role of CDK5 and Polo-like kinase 2 in homeostatic synaptic plasticity during elevated activity. Neuron *58*, 571–583.

Sheng, Z.H., Rettig, J., Takahashi, M., and Catterall, W.A. (1994). Identification of a syntaxin-binding site on N-type calcium channels. Neuron *13*, 1303–1313.

Sheng, Z.H., Westenbroek, R.E., and Catterall, W.A. (1998). Physical link and functional coupling of presynaptic calcium channels and the synaptic vesicle docking/fusion machinery. J. Bioenerg. Biomembr. *30*, 335–345.

Snutch, T.P. (2005). Targeting chronic and neuropathic pain: the N-type calcium channel comes of age. NeuroRx *2*, 662–670.

Su, S.C., and Tsai, L.H. (2011). Cyclin-dependent kinases in brain development and disease. Annu. Rev. Cell Dev. Biol. *27*, 465–491.

Swartz, K.J., Merritt, A., Bean, B.P., and Lovinger, D.M. (1993). Protein kinase C modulates glutamate receptor inhibition of Ca²⁺ channels and synaptic transmission. Nature *361*, 165–168.

Tan, T.C., Valova, V.A., Malladi, C.S., Graham, M.E., Berven, L.A., Jupp, O.J., Hansra, G., McClure, S.J., Sarcevic, B., Boadle, R.A., et al. (2003). Cdk5 is essential for synaptic vesicle endocytosis. Nat. Cell Biol. *5*, 701–710.

Tomizawa, K., Ohta, J., Matsushita, M., Moriwaki, A., Li, S.T., Takei, K., and Matsui, H. (2002). Cdk5/p35 regulates neurotransmitter release through phosphorylation and downregulation of P/Q-type voltage-dependent calcium channel activity. J. Neurosci. *22*, 2590–2597.

Tsai, L.H., Delalle, I., Caviness, V.S., Jr., Chae, T., and Harlow, E. (1994). p35 is a neural-specific regulatory subunit of cyclin-dependent kinase 5. Nature *371*, 419–423.

Viard, P., Butcher, A.J., Halet, G., Davies, A., Nürnberg, B., Heblich, F., and Dolphin, A.C. (2004). PI3K promotes voltage-dependent calcium channel trafficking to the plasma membrane. Nat. Neurosci. *7*, 939–946.

Weiss, N., Sandoval, A., Kyonaka, S., Felix, R., Mori, Y., and De Waard, M. (2011). Rim1 modulates direct G-protein regulation of Ca(v)2.2 channels. Pflugers Arch. *461*, 447–459.

Westenbroek, R.E., Hell, J.W., Warner, C., Dubel, S.J., Snutch, T.P., and Catterall, W.A. (1992). Biochemical properties and subcellular distribution of an N-type calcium channel α 1 subunit. Neuron *9*, 1099–1115.

Wheeler, D.B., Randall, A., and Tsien, R.W. (1994). Roles of N-type and Q-type Ca²⁺ channels in supporting hippocampal synaptic transmission. Science *264*, 107–111.

Yan, Z., Chi, P., Bibb, J.A., Ryan, T.A., and Greengard, P. (2002). Roscovitine: a novel regulator of P/Q-type calcium channels and transmitter release in central neurons. J. Physiol. *540*, 761–770.

Yarotskyy, V., and Elmslie, K.S. (2007). Roscovitine, a cyclin-dependent kinase inhibitor, affects several gating mechanisms to inhibit cardiac L-type (Ca(V)1.2) calcium channels. Br. J. Pharmacol. *152*, 386–395.

Yokoyama, C.T., Sheng, Z.H., and Catterall, W.A. (1997). Phosphorylation of the synaptic protein interaction site on N-type calcium channels inhibits interactions with SNARE proteins. J. Neurosci. *17*, 6929–6938.

Zamponi, G.W., Bourinet, E., Nelson, D., Nargeot, J., and Snutch, T.P. (1997). Crosstalk between G proteins and protein kinase C mediated by the calcium channel α1 subunit. Nature *385*, 442–446.

Zhu, L.Q., Liu, D., Hu, J., Cheng, J., Wang, S.H., Wang, Q., Wang, F., Chen, J.G., and Wang, J.Z. (2010). GSK-3 β inhibits presynaptic vesicle exocytosis by phosphorylating P/Q-type calcium channel and interrupting SNARE complex formation. J. Neurosci. *30*, 3624–3633.

Zucker, R.S., and Regehr, W.G. (2002). Short-term synaptic plasticity. Annu. Rev. Physiol. *64*, 355–405.